ORIGINAL ARTICLE

Deep RNA Sequencing Revealed Fusion Junctional Heterogeneity May Predict Crizotinib Treatment Efficacy in *ALK*-Rearranged NSCLC

Zhengbo Song, MD, PhD,[a,b] Shifeng Lian, MD, MSc,[c] Silvia Mak, MSc,[d] Maggie Zi-Ying Chow, PhD,[d] Chunwei Xu, MD,[e] Wenxian Wang, MD,[a,b] Hoi Yee Keung, PhD,[b] Chenyu Lu, MSc,[f,g] Firaol Tamiru Kebede, PhD,[f] Yanqiu Gao, BSc,[h] Wah Cheuk, MD, PhD,[i] William Chi Shing Cho, PhD,[j] Mengsu Yang, PhD,[f,g] Zongli Zheng, PhD[d,f,g,*]

[a]*Department of Clinical Trial, The Cancer Hospital of the University of Chinese Academy of Sciences (Zhejiang Cancer Hospital), Hangzhou, Zhejiang, People's Republic of China*
[b]*Institute of Basic Medicine and Cancer, Chinese Academy of Sciences, Hangzhou, Zhejiang, People's Republic of China*
[c]*Unit of Integrative Epidemiology, Institute of Environmental Medicine, Karolinska Institutet, Stockholm, Sweden*
[d]*Ming Wai Lau Centre for Reparative Medicine, Karolinska Institutet, Sha Tin, Hong Kong Special Administrative Region of the People's Republic of China*
[e]*Department of Respiratory Medicine, Jinling Hospital, Nanjing University School of Medicine, Nanjing, People's Republic of China*
[f]*Department of Biomedical Sciences, City University of Hong Kong, Kowloon, Hong Kong Special Administrative Region of the People's Republic of China*
[g]*Biotechnology and Health Centre, City University of Hong Kong Shenzhen Research Institute, Shenzhen, People's Republic of China*
[h]*Helitec Limited, Shenzhen, People's Republic of China*
[i]*Department of Pathology, Queen Elizabeth Hospital, Kowloon, Hong Kong Special Administrative Region of the People's Republic of China*
[j]*Department of Clinical Oncology, Queen Elizabeth Hospital, Kowloon, Hong Kong Special Administrative Region of the People's Republic of China*

Received 18 June 2021; revised 13 September 2021; accepted 18 September 2021
Available online - XXX

ABSTRACT

Introduction: Gene fusion variants in *ALK*-rearranged NSCLC may predict patient outcomes, but previous results have been inconclusive. Fusion isoforms coexisting in the same tumor may affect the efficacy of targeted therapy, but they have not been investigated.

Methods: Patients with *ALK*-rearranged NSCLC who received crizotinib treatments were recruited. Precrizotinib tumor tissues were analyzed by the anchored multiplex polymerase chain reaction for targeted RNA sequencing. Kaplan-Meier and Cox regression were used to compare overall and progression-free survivals.

Results: Of the 51 studied subjects, *EML4-ALK* variant types v1, v2, v3, and others were detected in 23 (45.1%), five (9.8%), 19 (37.3%), and four patients (7.8%), respectively. Multiple *EML4-ALK* RNA isoforms were detected in 24 tumors (47.1%), and single isoform in 27 (52.9%). Most of the v3 tumors (16 of 19) harbored both v3a and v3b RNA isoforms. Multiple isoforms were also detected in eight non-v3 tumors (33.3% of all 24 multiple isoforms; five v1, two v5′, and one v2). Compared with patients with single isoform, those with multiple isoforms had worse progression-free (hazard ratio and 95% confidence interval:

*Corresponding author.

Drs. Song, Lian, Mak, and Chow contributed equally to this work.

Disclosure: Dr. Zheng held equity in ArcherDX, a licensee of the AMP technology from Massachusetts General Hospital. Drs. Zheng and Yang were scientific advisors for and held equity in Helitec Limited, which interests were reviewed and regulated by institutional Outside Practice and Outside Work policies annually. Dr. Gao was employed at Helitec Limited. The remaining authors declare no conflict of interest.

Address for correspondence: Zongli Zheng, PhD, Department of Biomedical Sciences, City University of Hong Kong, Kowloon, Hong Kong Special Administrative Region of the People's Republic of China. E-mail: zongli.zheng@cityu.edu.hk

ISSN: 1556-0864
https://doi.org/10.1016/j.jtho.2021.09.016

2.45 [1.06–5.69]) and overall (hazard ratio [95% confidence interval]: 3.74 [1.26–11.13]) survivals after adjusting for potential confounders including variant type. Using the patient-derived H2228 cells known to express v3a and v3b, our single-cell polymerase chain reaction detected either v3a or v3b in most single cells. Treatment of H2228 cells by three ALK inhibitors revealed increased ratios of v3a-to-v3b expression over time.

Conclusions: Intratumoral *EML4-ALK* isoforms may predict the efficacy of targeted therapy in *ALK*-rearranged NSCLC. Temporal changes of intratumoral fusion isoforms may result from differential selection pressures that a drug might have on one isoform over another. Larger studies on fusion heterogeneity using RNA sequencing are warranted.

Keywords: RNA sequencing; ALK fusion heterogeneity; Fusion isoforms; Crizotinib; ALK TKI

Introduction

Tumors carrying the same driver genes may respond differently to the same targeted therapy drug. Among *ALK*-rearranged NSCLC,[1] there were considerable advances with several generations of *ALK* tyrosine kinase inhibitors (TKIs).[2] Nevertheless, one of the major fusion variants—*EML4-ALK* variant 3 (v3; *EML4* exon 6 fused to *ALK* exon 20)—has been associated with less favorable clinical outcomes compared with patients with other fusion variants.[3–7] Numerical differences in progression-free survival (PFS) after crizotinib or brigatinib between *EML4-ALK* variants have been observed in the first-line randomized phase 3 trial.[7,8] Of note, the ALEX study used a DNA-based method to detect genomic changes. However, owing at least partially to passenger fusions,[9] genomic breakpoints may or may not accurately predict spliced transcripts that are productive of driver oncoproteins.[9,10] Furthermore, within the same gene-gene fusion partners, genomic breakpoints may be unreliable predictors of splicing variants, as indeed found in *ROS1* gene fusions.[11] In contrast, protein stabilities of various *EML4-ALK* fusion variants have been suggested as one possible explanation for the difference in variant-related drug response.[12] Lastly, clinical sequencing has documented an ever-expending catalog of dual gene partners fused in frame with 3′ ALK.[13]

Targeted therapy is often limited by eventual cancer resistance. Diverse mechanisms of resistance in ALK targeted therapy have been identified, including kinase domain mutations, amplifications, and ALK-independent signaling pathway activations.[14] The fusion v3 tumor has been found to be associated with the development of resistance mutations, in particular G1202R.[6] Tumor heterogeneity—as the underlining mechanism for cancer resistance—has been evaluated largely for cases with multigene polyclonal alterations.[14,15] Yet, for multiple *EML4-ALK* transcript isoforms that coexist in the same tumor,[16] which could be a result of either multiple genomic-level breakpoints or alternative splicing, to our knowledge, it has not been investigated with regard to their clinical relevance and inhibition resistance.

To study whether *ALK* fusion heterogeneity is related with clinical outcomes in patients with NSCLC, we performed a retrospective analysis among patients with *ALK*-rearranged NSCLC who received crizotinib treatment. We used the anchored multiplex polymerase chain reaction (PCR)[16] method for targeted RNA sequencing (RNA-seq) that is not limited to specific fusion variants or gene partners, for the characterization of fusion heterogeneity in formalin-fixed paraffin-embedded (FFPE) tumor tissues and in culture cells. We further conducted single-cell reverse-transcriptase PCR (RT-PCR) and in vitro TKI inhibition experiments to evaluate the effect of fusion heterogeneity on drug response.

Materials and Methods

Baseline Clinical Characteristics of Study Patients

The study included patients with the following criteria: (1) diagnosed with having stage IV NSCLC and hospitalized in The Cancer Hospital of the University of Chinese Academy of Sciences (Zhejiang Cancer Hospital) between November 1, 2013, and April 30, 2019; (2) positive for having *ALK* fusions according to our clinical fluorescence in situ hybridization (four cases, positive cells range 28%–40%), immunohistochemistry (VENTANA ALK D5F3 CDx Assay, three cases), or RT-PCR (AmoyDx *EML4-ALK* (2013/3400389), 44 cases) assays; (3) TKI naive before receiving crizotinib treatments; (4) Eastern Cooperative Oncology Group (ECOG) performance scores of 0 or 1; and (5) available FFPE tissues for RNA and DNA sequencing. The end date of follow-up was December 31, 2020. All participants provided written informed consent. The study was approved by institutional review board at The Cancer Hospital of the University of Chinese Academy of Sciences, People's Republic of China.

Gene Fusion Detection and Variant Quantification Using Next-Generation Sequencing

Total nucleic acids (TNAs) containing RNA and DNA were extracted from FFPE sections using the Agencourt FormaPure Kit (Beckman Coulter, Indianapolis, IN) or

PANO-Pure for FFPE TNA Extraction Kit (Helitec Biotechnologies, Shenzhen, People's Republic of China). After quantification by Qubit HS RNA Assay Kits (Thermo Fisher Scientific, Waltham, MA), 50 ng of TNA was used for next-generation sequencing (NGS) library preparation. Briefly, targeted NGS libraries were constructed using the anchored multiplex PCR method,[16] with modifications including the incorporation of an unique molecular identifier (UMI) in the adaptor and using a one-tube enrichment of RNA and DNA targets in 62 genes as described previously.[17,18] The libraries were then quantitated by quantitative PCR (qPCR) and sequenced on Illumina HiSeq X10 or NovaSeq System. Raw FASTQ data were trimmed for adaptors using BBduk[19] and parsed for UMI using a custom script. Gene fusions were called using the SplitFusion algorithm developed initially on the basis of the BLAT genome reference mapping[20] and validated[16] and redesigned on the basis of the fast aligner BWA MEM[21] with new features (https://github.com/Zheng-NGS-Lab/SplitFusion). To quantify the relative abundance of v3a to v3b reads, UMI-consolidated BAM files were used to count the numbers of v3a and v3b reads, respectively. The ratio of the two numbers (v3a–v3b) was calculated.

Reverse Transcription and qPCR Quantification of v3a and v3b Variants

Reverse transcription was performed according to the manufacturer's protocol (18064014, Invitrogen, Waltham, MA). In brief, 150 ng of random hexamer, 1 μL of 10 mM dNTPs, and 1 μg of RNA were topped up to 12 μL with nuclease-free water and incubated at 65°C for 5 minutes followed by a quick chill on ice. Then, 1× first-stand buffer, 0.01 M dithiothreitol, and 40 U of RNaseOUT (10777019, Invitrogen) were added into the mix. After a 2-minute incubation at 25°C, 1 μL of SuperScript II reverse transcriptase was added followed by an incubation of 25°C for 10 minutes, 42°C for 50 minutes, and 70°C for 15 minutes. The complementary DNA samples were stored at −20°C until use. The qPCR quantification was performed by using PrimeTime Gene Expression Master Mix (1055771, Integrated DNA Technologies, Coralville, IA). Each qPCR reaction was 20 μL containing 1× Gene Expression Master Mix, 0.5 μM forward primer (GTCGAAAATACCTTCAACACC), 0.5 μM reverse primer (TTGCTCAGCTTGTACTCAGG), 0.3 μM TaqMan probe (v3a: 5′-JOE-CCAAAACTGCAGACAAGCATAAAGATG-MGB-3′; v3b: 5′-FAM-TGTCAACTCGCGAAAAAAACAGC-MGB-3′; GENEWIZ, Suzhou, People's Republic of China), and 1 μL of complementary DNA from reverse transcription described previously. The thermocycling condition was 95°C for 3 minutes, followed by 40 cycles at 95°C for 15 seconds, and 60°C for 1 minute. The expression of housekeeping gene *CHMP2A* was included for normalization control (forward primer: CAC TCAAGTCCAACAACTCGA, reverse primer: GCCGCTCAAA CTCCATCATG, probe: /5 6-FAM/ CCATGGCCT/ZEN/TGG TGACACCCTTCAT/3 IABkFQ/; IDTDNA Technologies, Singapore).

Cell Culture and ALK Inhibitor Treatment

The H2228 cell line (NCI-H2228, American Type Culture Collection, Manassas, VA) was cultured using Roswell Park Memorial Institute 1640 supplemented with 10% fetal bovine serum (10270106, Gibco, Amarillo, TX) at 37°C in a humidified 5% CO_2 incubator. Crizotinib (PZ0191) was purchased from Sigma-Aldrich (Darmstadt, Germany), whereas ceritinib (A126440) and alectinib (A264992) were purchased from AmBeed (Arlington Heights, IL). Stock solutions were prepared in DMSO and were further diluted in complete growth medium before adding into the cells. The final DMSO concentration was less than 0.1% in the cell culture medium. Stock solutions were stored at −20°C. In ALK inhibitor treatments, H2228 cells were exposed to 500 nM of crizotinib, ceritinib, or alectinib and passaged once a week. Approximately 1×10^6 cells were collected for DNA and RNA extraction using AllPrep DNA/RNA Mini Kit (80204, Qiagen, Hilden, Germany) for downstream NGS library construction.

Cell Viability Assay

Cells were seeded in 96-well plates at 2.5×10^3 cells per well and were treated with 500 nM of crizotinib, ceritinib, or alectinib for 72 hours or longer. The cell viability was performed using Cell Proliferation Kit II (XTT) (11465015001, Sigma-Aldrich) according to the manufacturer's instruction. Briefly, XTT labeling reagent and electron-coupling reagent were thawed in a 37°C water bath just before use. XTT labeling reagent and electron-coupling reagent were mixed in a ratio of 50:1. Then, 50 μL of the working solution was added into each well and incubated at 37°C with 5% CO_2 in a humidified atmosphere for 2 hours. Cell viability was then determined by the absorbance at 450 nm.

Direct Single-Cell RT-PCR

H2228 cells were resuspended in 1× PBS with 0.05% bovine serum albumin (A3733, Sigma-Aldrich) and diluted to a final concentration of 1 cell/μL. Each aliquot of 1 μL of the diluted cell resuspension was added into one PCR tube and incubated at room temperature for 5 minutes in 1 μL of freshly made lysis buffer, which contained 1% NP-40 (ab142227, Abcam), 0.1% bovine serum albumin, and 5 U RNaseOUT (10777019, Invitrogen). Reverse transcription and

amplification of EML4-ALK transcript were performed using SuperScript IV One-Step RT-PCR System (12594100, Invitrogen), in which 1× Platinum SuperFi RT-PCR Master Mix, 0.2 μL of SuperScript IV room temperature mix, 0.4 μM each of forward and reverse primers (Fw′-GTGACTGGAGTTCAGACGTGTGCTCTTC-CGATCTATTGTCGAAAATACCTTCAACACCCA; Rv′-CCTA-CACGACGCTCTTCCGATCTCATCTGCATGGCTTGCAGCTCC), and 15 U RNaseOUT were added to a final volume of 20 μL with nuclease-free water in each RT-PCR reaction. The thermocycling condition was as follows: 55°C for 10 minutes (reverse transcription), and then 98°C for 2 minutes (room temperature inactivation and initial denaturation), followed by 40 cycles at 98°C for 10 seconds, 60°C for 10 seconds, and 72°C for 30 seconds, with a final extension step at 72°C for 5 minutes.

Statistical Analysis

Patient baseline characteristics were compared between groups using Fisher's exact test for categorical variables and analysis of variance for continuous variables. The Kaplan-Meier method and log-rank test were used to compare PFS and overall survival (OS) curves. Cox proportional hazards regression was used to calculate hazard ratios (HRs) with 95% confidence interval (CI). Stratified and multivariate regression analyses were used to control for potential confounders, including sex, age, ECOG score, smoking, brain metastasis, variant type, and isoform number. All statistical analyses were performed using the Statistical Analysis System software (version 9.4, SAS Institute, Cary, NC).

Results

Baseline Characteristics of the Study Patients

We recruited 51 patients with NSCLC who fulfilled our inclusion criteria, and prognoses were followed up until December 31, 2020. The cohort included 33 females (65.0%) and 18 males (35.0%), with a mean age of 53.8 (range: 29–76) years at diagnosis (Table 1). The ECOG performance score was 0 for 37.3% of the patients and 1 for the rest. There were 21.6% smokers, and 33.3% of the patients had brain metastasis.

Table 1. Baseline Clinicopathologic Characteristics of *EML4-ALK* Fusion-Positive Patients Included in This Study, by Fusion Variant Type (v3/Non-v3) and Number of Isoforms

		EML4-ALK Variant			Number of *EML4-ALK* Isoforms		
Variable	All	Non-v3	V3	*p* Value	1	≥ 2	*p* Value
Patients, n (%)	51	32 (62.7)	19 (37.3)		27 (52.9)	24 (47.1)	
Mean age, y (range)	53.8 (29-76)	55.0 (29-76)	51.6 (31-67)	0.340	54.9 (29-76)	52.5 (31-67)	0.490
Sex, n (%)							
Female	33 (65.0)	20	13	0.669	16	17	0.388
Male	18 (35.0)	12	6		11	7	
ECOG score, n (%)							
0	19 (37.3)	12	7	0.963	12	7	0.260
1	32 (62.7)	20	12		15	17	
Smoking, n (%)							
No	40 (78.4)	24	16	0.439	20	20	0.422
Yes	11 (21.6)	8	3		7	4	
Brain metastasis, n (%)							
No	34 (66.7)	22	12	0.682	18	16	1.000
Yes	17 (33.3)	10	7		9	8	
EML4-ALK variant,[a] n (%)							
V3 (exon 6)	19 (37.3)	–	–		3	16	<0.001
V3a only		–	1 (2.0)		1	0	
V3a and v3b		–	16 (31.4)		0	16	
V3b only		–	2 (3.9)		2	0	
Non-v3	32 (62.7)	–	–		24	8	
V1 (exon 13)		23 (45.1)	–		18	5	
V2 (exon 20)		5 (9.8)	–		4	1	
V5′ (exon 18)		3 (5.9)	–		1	2	
V5 (exon 2)		1 (2.0)	–		1	0	

Note: The number of *EML4-ALK* isoforms was defined by the number of breakpoints inferred in RNA sequencing reads.
[a]For cases with multiple isoforms involving different exons, only the dominant isoform exon is listed in the table (Supplementary Table 1 for the detailed list of all isoforms).
ECOG, Eastern Cooperative Oncology Group.

EML4-ALK Variant Type and Isoform Number

Using our one-tube RNA and DNA sequencing method, we detected various *EML4-ALK* variant types in our study cohort. Two dominant variants were v1 (n = 23; 45.1%) and v3 (n = 19; 37.3%), and less frequent variants were v2 (n = 5; 9.8%), v5′ (n = 3; 5.9%) and v5 (n = 1; 2.0%) (Table 1). Multiple *EML4-ALK* isoforms were detected in 24 tumors (47.1%) (full list in Supplementary Table 1), and single isoform in 27 tumors (52.9%). Most (16 of 19, 84.2%) of the v3 tumors harbored both v3a (involving *EML4* exon 6) and v3b (involving *EML4* exon 6 plus a cryptic exon of 33 bases) transcript isoforms (Fig. 1*A* and *B*). Detailed breakpoints of all isoforms were inferred from split-read mapping and reported by SplitFusion (Fig. 1*C*). The percentage of dominant isoform in one sample ranged from 53.1% to 99.8% (Fig. 1*D* and Supplementary Table 1). One patient had v3a only, and two patients had v3b only (Table 1). Multiple-isoform tumors were more frequent in v3 tumor than in non-v3 tumors ($p < 0.001$). In contrast, multiple isoforms existed in eight non-v3 tumors (five v1, two v5′, and one v2), consisting of 33.3% of the total 24 multiple-isoform tumors. Patient baseline characteristics were balanced between v3 and non-v3 groups and between single- and multiple-isoform groups (Table 1).

EML4-ALK Variant Type, Isoform Number, and PFS

We first compared PFSs after crizotinib treatment by fusion variant type and isoform number. The difference in PFSs of patients with and without v3 was not statistically significant (median PFS =8.9 mo versus 13.8 mo, $p = 0.082$; Fig. 2*A*). The PFS in patients with multiple isoforms was significantly shorter than that of patients with single isoform (median PFS = 8.9 mo versus 15.9 mo, $p = 0.006$; Fig. 2*B*). Because variant type was associated with isoform number, to control for the possible effect of variant type that may have on the association between isoform number and PFS and vice versa, we further performed stratified analyses. Then, because there were only three cases that belong to the v3 single-isoform group, we did not include comparisons with this group. The results revealed that, among the multiple-isoform group, there was no difference in PFSs between the multiple-isoform v3 and multiple-isoform non-v3 groups (median PFS = 9.0 mo versus 7.6 mo; $p = 0.928$; Fig. 2*C*). In contrast, among the non-v3 group, patients with multiple isoforms had shorter PFS than those with single isoform (median PFS = 7.6 mo versus 15.9 mo; $p = 0.045$; Fig. 2*D*).

Univariate and Multivariate Cox Regression Analyses for Factors Related With PFS

In Cox regression analyses, the PFS in the v3 group was not different from that of the non-v3 group in univariate model (HR [95% CI]: 1.72 [0.93–3.18]) nor in multivariate model (HR [95% CI]: 1.05 [0.45–2.43]) (Table 2). In contrast, PFS was worse in the multiple-isoform group when compared with the single-isoform group, with statistically significant difference in the univariate model (HR [95% CI]: 2.37 [1.26–4.45]; Table 2) and in the multivariate model after adjustments for potential confounders (HR [95% CI]: 2.45 [1.06–5.69]). In stratified analyses, among the patients with multiple isoforms, the v3 variant type was not associated with PFS (HR [95% CI]: univariate 0.96 [0.37–2.48] and multivariate 1.03 [0.35–3.08]) (Table 2). Consistent with the Kaplan-Meier analysis, among patients without v3, multiple isoform was associated with a worse PFS compared with single isoform (HR [95% CI]: univariate 2.44 [0.99–6.02] and multivariate 3.68 [1.21–11.21]) (Table 2).

EML4-ALK Variant Type, Isoform Number, and OS

We then compared OSs of patients with *ALK*-rearranged NSCLC by variant type and isoform number. The patients with v3 had shorter OS than those without, but the difference did not reach statistical significance (median OS = 21.6 mo versus 38.5 mo, $p = 0.149$; Fig. 3*A*). Patients with multiple-isoform tumors had shorter OS than patients with single-isoform tumors (median OS = 18.5 mo versus 49.8 mo; $p = 0.016$; Fig. 3*B*). In stratified analyses, among the patients with multiple-isoform tumors, fusion variant type was not associated with OS (median OS v3 versus non-v3 = 21.6 mo versus 16.5 mo; $p = 0.257$; Fig. 3*C*). Nevertheless, multiple isoform was associated with a shorter OS than single isoform among the patients without v3 (median OS = 16.5 mo versus 49.8 mo; $p = 0.003$; Fig. 3*D*).

Univariate and Multivariate Cox Regression Analyses for Factors Related With OS

In univariate Cox regression, the only baseline clinical characteristic associated with OS was age (HR [95% CI]: 1.04 [1.01–1.07]; Table 2). The OS of patients with v3 was not different from that of patients without v3 before (HR [95% CI]: 1.73 [0.82–3.65]) nor after adjustment for potential confounders (HR [95% CI]: 1.06 [0.39–2.87]). Meanwhile, multiple isoform was associated with excess risk of death compared with single isoform before and after adjusting for potential confounders (HR [95% CI]: 2.46 [1.16–5.22] and 3.74 [1.26–11.13]). In stratified analyses, the fusion variant type was not associated with PFS (HR [95% CI]: univariate 0.57 [0.21–1.53] and multivariate 0.67 [0.21–2.16]). Among the non-v3 group, multiple isoform was associated with excess risk of death compared with single isoform (HR [95% CI]: 4.24 [1.52–11.80]) in univariate and multivariate models after adjusting for potential confounders (HR [95% CI]: 12.56 [2.87–54.98]).

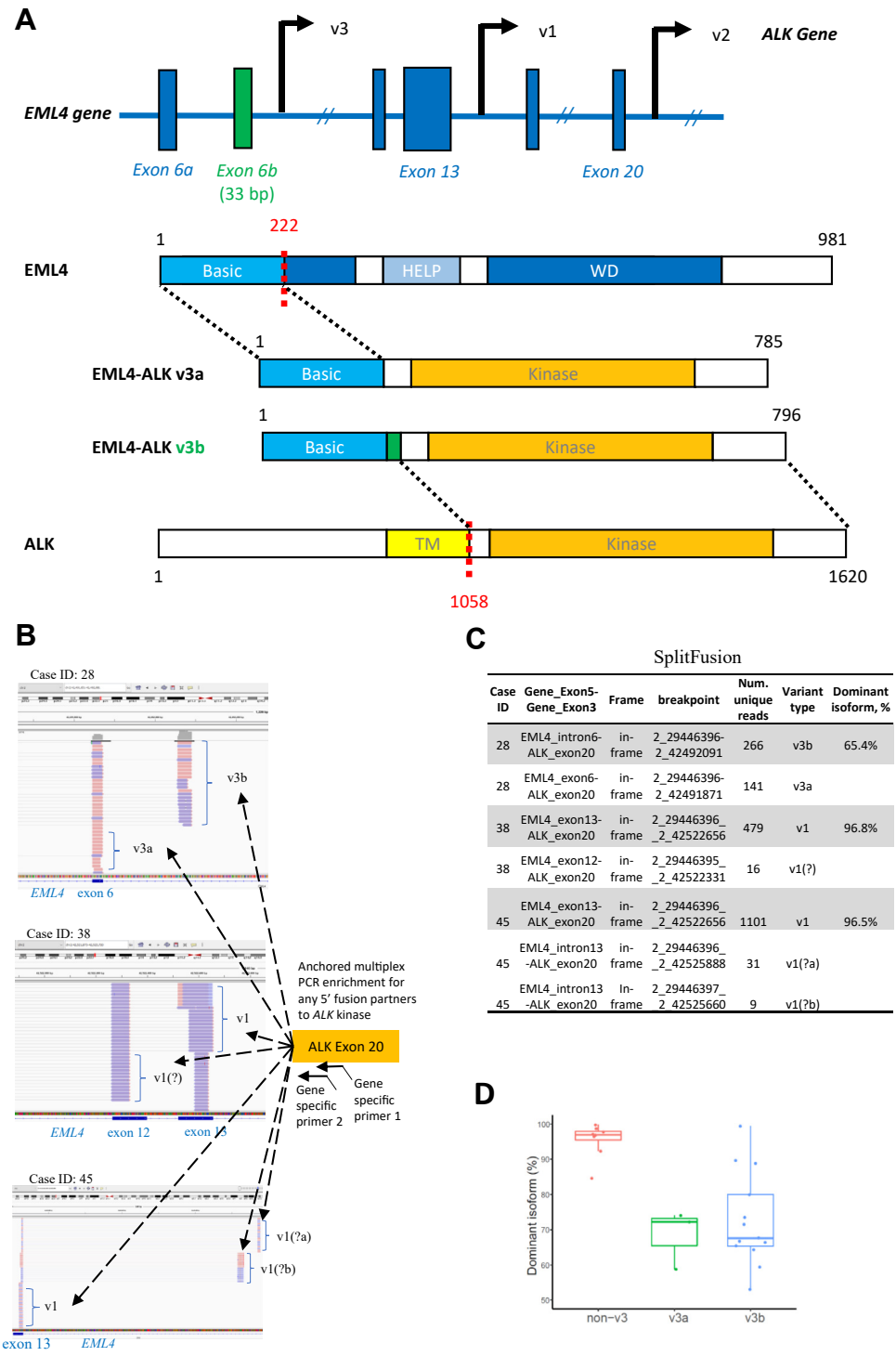

Case ID	Gene_Exon5-Gene_Exon3	Frame	breakpoint	Num. unique reads	Variant type	Dominant isoform, %
28	EML4_intron6-ALK_exon20	in-frame	2_29446396-2_42492091	266	v3b	65.4%
28	EML4_exon6-ALK_exon20	in-frame	2_29446396-2_42491871	141	v3a	
38	EML4_exon13-ALK_exon20	in-frame	2_29446396_-2_42522656	479	v1	96.8%
38	EML4_exon12-ALK_exon20	in-frame	2_29446395_-2_42522331	16	v1(?)	
45	EML4_exon13-ALK_exon20	in-frame	2_29446396_-2_42522656	1101	v1	96.5%
45	EML4_intron13-ALK_exon20	in-frame	2_29446396_-2_42525888	31	v1(?a)	
45	EML4_intron13-ALK_exon20	In-frame	2_29446397_-2_42525660	9	v1(?b)	

Figure 1. (*A*) Schematic presentations of *EML4-ALK* fusion variant breakpoints and the variants 3a and 3b. Example visualization of genome mapping using IGV for three NSCLC cases with coexisting isoforms using anchored multiplex PCR to target *ALK* kinase exon 20 for any 5′ fusion partners (arrows indicated the heminested gene-specific primers). Case #28 contained two isoforms v3a and v3b. The v3b was formed by splicing of a cryptic exon in classic *EML4* intron 6. Case #38 contained the dominant isoform v1 and minor v1(?). The minor isoform v1(?) revealed a breakpoint in the middle of *EML4* exon 12. Case #45 contained the dominant v1 and two minor isoforms v1(?a) and v1(?b). (*B*) The two minor isoforms were formed by splicing of two cryptic exons in classic *EML4* intron 13, respectively. Example SplitFusion output results for the cases. The chromosomal breakpoints were inferred from cDNA and using human reference genome build hg19. (*C*) The proportion of the dominant isoform supporting reads among all fusion reads were indicated. (*D*) The distributions of dominant isoform percentage in each sample for all 24 samples with multiple isoforms by variant types (non-v3, v3a, and v3b). #, number; bp, base pair; cDNA, complementary DNA; ID, identification; IGV, Integrative Genomics Viewer; Num., number; PCR, polymerase chain reaction.

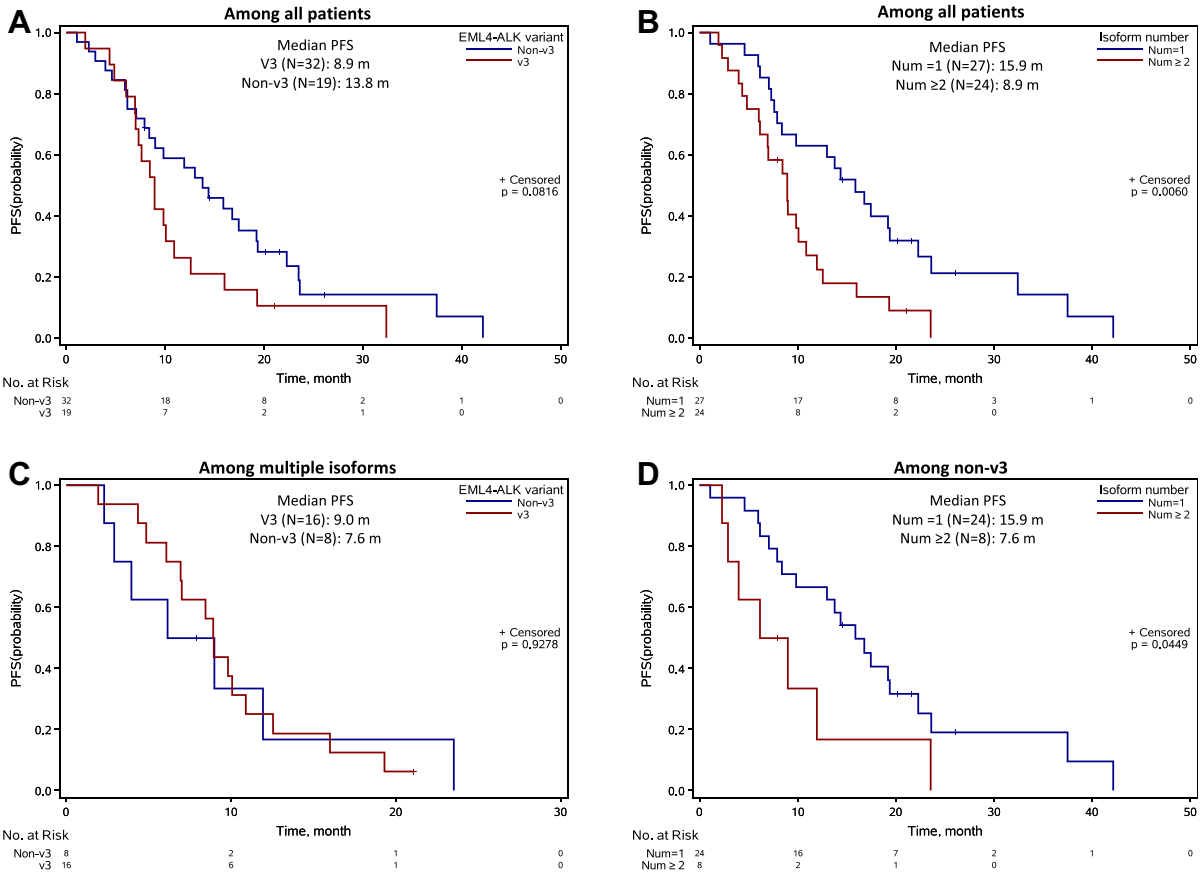

Figure 2. Kaplan-Meier curves comparing PFSs among patients with *EML4-ALK* NSCLC by the fusion variant type (*[A]* v3 versus non-v3) and number of isoforms (*[B]* single versus multiple). Stratification analyses were further performed (*C*) to compare PFSs of the fusion variant types among patients with multiple isoforms and (*D*) to compare PFSs of different number of isoforms among patients with non-v3 *EML4-ALK* tumors. Num, number; PFS, progression-free survival.

In Vitro Study of the Inhibition of Three ALK Inhibitors on H2228 Cell Line

To evaluate the efficacy of ALK TKIs in cell viability of v3a- and v3b-expressing cells, in vitro experiments were carried out in H2228 cells. The H2228 cells with *EML4-ALK* v3 fusions were treated with three different TKIs, namely crizotinib, ceritinib, and alectinib, for 3 weeks. After each week, cell viabilities were measured using the XTT. Three TKI treatments resulted in 52% to 72% decrease in cell viability compared with untreated control at week 1, 43% to 76% decrease at week 2, and 24% to 69% decrease at week 3 (Fig. 4*A*). NGS analyses were also performed for the investigation of how TKIs affect v3a and v3b variants in the cell population. Interestingly, after 1, 2, and 3 weeks of treatment, increasing v3a-to-v3b ratios were observed in all three TKI-treated groups compared with the untreated control group: crizotinib from 1.57 to 1.94 and 2.52, ceritinib from 1.26 to 2.84 and 2.85, and alectinib from 1.69 to 1.92 and 2.48, respectively (Fig. 4*B*). The results were confirmed by RT-qPCR using v3a- and v3b-specific TaqMan probes, except a slightly decrease ratio observed in alectinib treatment after 2 weeks (Fig. 4*C* and *D*).

Single-Cell Study on Alternative RNA Splicing

The above-mentioned observation of enrichment of v3a relative to v3b RNA expression suggested that the v3a-expressing cells might be more resistant to TKI inhibitors. To study whether v3a and v3b variants are characteristic of single cells or whether the variants coexist in the same cell owing to stochastic expression of the two isoforms, we performed a single-cell RT-PCR experiment to amplify the v3a and v3b mRNAs using the same set of PCR primers. First, at approximately 50 cells per reaction, all eight reactions revealed two amplicon bands (v3b is 33 base pair longer than v3a; Fig. 4*E*). Next, to achieve single-cell target amplification, we performed a limited dilution to approximately one cell per reaction well across 48 wells (Fig. 4*F*). The reason we chose one cell per well was because, according to Poisson distribution, when λ (the expected rate of occurrence) is 1, the probabilities of getting 0, 1, and greater than or equal to 2 cells per well are 0.3679, 0.3679, and

Table 2. Cox Regression Analyses of Factors Related With PFS and OS Among Patients With *EML4-ALK* NSCLC

		PFS		OS	
	Patient	Univariate	Multivariate	Univariate	Multivariate
Variable	N	HR (95% CI)	HR (95% CI)	HR (95% CI)	HR (95% CI)
Age, y (range)	51	1.012 (0.987-1.037)	1.021 (0.99-1.053)	1.04 (1.006-1.074)	1.067 (1.022-1.115)
Sex					
Female	33	1.0 (reference)	1.0 (reference)	1.0 (reference)	1.0 (reference)
Male	18	1.588 (0.848-2.975)	1.574 (0.635-3.901)	1.256 (0.581-2.716)	2.641 (0.94-7.418)
ECOG					
0	19	1.0 (reference)	1.0 (reference)	1.0 (reference)	1.0 (reference)
1	32	1.042 (0.56-1.94)	1.114 (0.532-2.333)	1.654 (0.73-3.75)	1.78 (0.701-4.524)
Smoking					
No	40	1.0 (reference)	1.0 (reference)	1.0 (reference)	1.0 (reference)
Yes	11	1.434 (0.694-2.961)	0.961 (0.342-2.7)	0.6 (0.206-1.749)	0.319 (0.082-1.243)
Brain metastasis					
No	34	1.0 (reference)	1.0 (reference)	1.0 (reference)	1.0 (reference)
Yes	17	1.252 (0.673-2.329)	1.426 (0.682-2.981)	1.295 (0.598-2.803)	2.17 (0.866-5.434)
EML4-ALK variant					
Non-v3	32	1.0 (reference)	1.0 (reference)	1.0 (reference)	1.0 (reference)
V3	19	1.717 (0.927-3.179)	1.045 (0.45-2.427)	1.725 (0.815-3.65)	1.057 (0.389-2.867)
Isoform number					
1	27	1.0 (reference)	1.0 (reference)	1.0 (reference)	1.0 (reference)
$\geq$ 2	24	2.366 (1.258-4.449)	2.451 (1.055-5.69)	2.457 (1.157-5.22)	3.738 (1.256-11.13)
Stratified analyses					
Among multiple isoforms, variant					
Non-v3	8	1.0 (reference)	1.0 (reference)	1.0 (reference)	1.0 (reference)
V3	16	0.957 (0.37-2.476)	1.032 (0.346-3.082)	0.566 (0.209-1.533)	0.666 (0.206-2.159)
Among non-v3, isoform number					
1	24	1.0 (reference)	1.0 (reference)	1.0 (reference)	1.0 (reference)
$\geq$ 2	8	2.442 (0.991-6.017)	3.683 (1.21-11.21)	4.239 (1.523-11.80)	12.56 (2.87-54.98)

Note: Univariate and multivariate Cox models were used to calculate HR and 95% CI. Stratification analyses were performed to compare fusion variant among patients with multiple isoforms and to compare isoform number among patients with non-v3 *EML4-ALK* fusions.
CI, confidence interval; ECOG, Eastern Cooperative Oncology Group; HR, hazard ratio; OS, overall survival; PFS, progression-free survival.

0.2642, respectively. A total of 48 reactions would yield substantial proportions of reactions with empty (expected 18 of 48), single (expected 18 of 48), and multiple (expected 13 of 48) amplicon bands. The results revealed that empty, single (v3a-only or v3b-only), and mixed bands were observed in 20, 16 (8 + 8), and 12 wells (Fig. 4*F*), respectively, consistent with the expected numbers by Poisson distribution (Fisher's exact test $p = 0.903$; Fig. 4*G*) and indicate truly single-cell amplification, similarly as what we have reported in single-molecule amplification and sequencing[22] and NGS.[23] The result indicated that the input cells contained mostly v3a-only or v3b-only RNA, instead of mostly mixed v3a and v3b RNAs that would be expected to yield both amplicon bands in most reactions.

Discussion

Gene fusion heterogeneity measured by coexisting multiple in-frame *EML4-ALK* transcript isoforms that translate into multiple protein variants in the same tumor, which presumably may have clinical relevance, is yet to be studied thus far. Our results from a post-crizotinib *ALK*-rearranged NSCLC cohort revealed that patients with multiple *EML4-ALK* RNA isoforms, compared with patients with single isoform, had worse OS and shorter PFS after crizotinib treatment. Most clinical v3 tumors were found to be heterogeneous and harbored mixed v3a and v3b fusion transcripts. Among those with non-v3 tumors, the fusion heterogeneity was also strongly associated with worse clinical outcomes. Previous observations of poor clinical outcomes in patients with *EML4-ALK* v3 may be, at least in part, explained by the effect of fusion heterogeneity, which needs to be confirmed in larger studies and the understanding of which would be relevant in designing future targeted therapy strategies.

We reported that nearly half of the patients with *EML4-ALK* NSCLC (47.1%) tumors harbored multiple *EML4-ALK* isoforms. Patients in this group had a

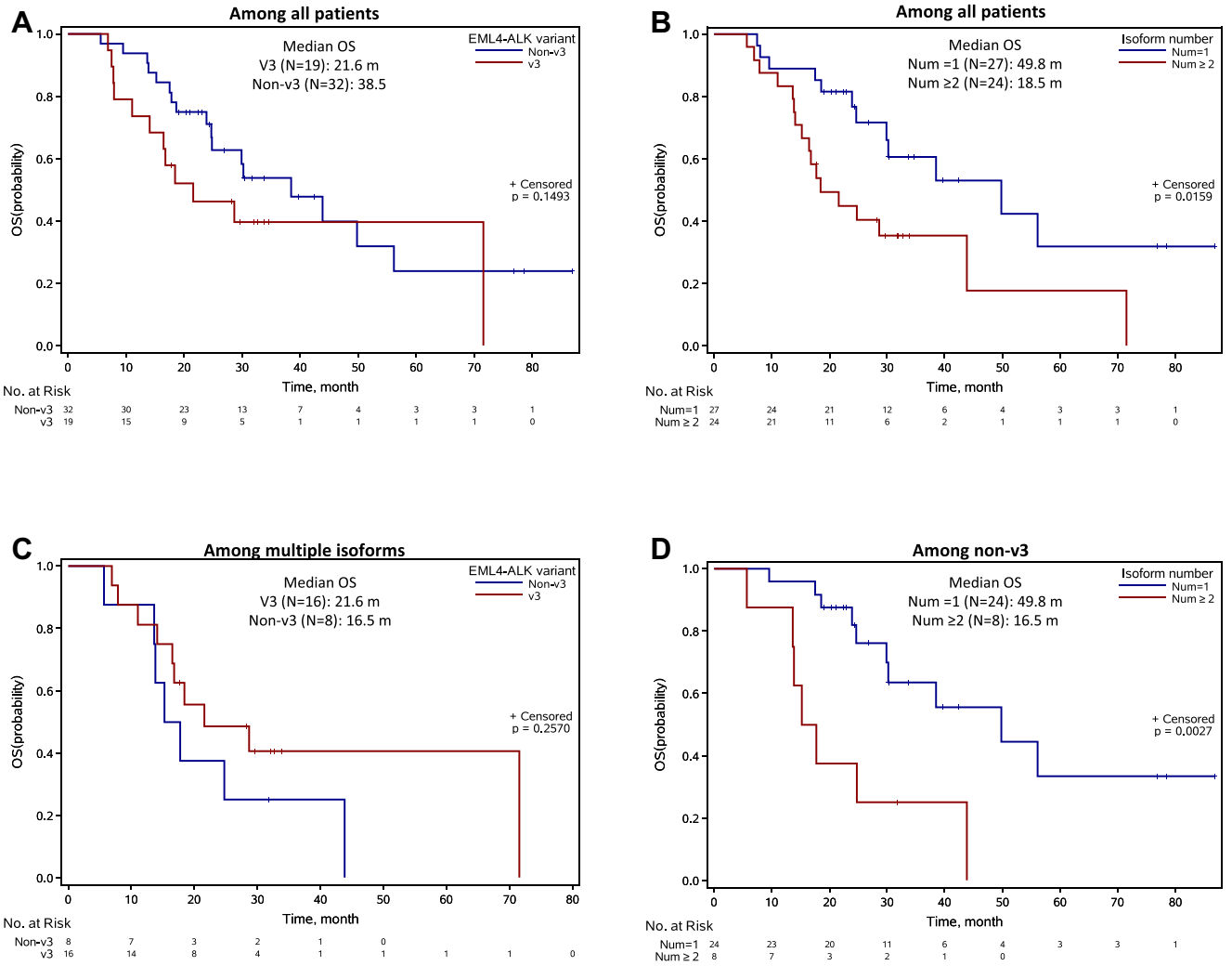

Figure 3. Kaplan-Meier curves comparing OSs among patients with *EML4-ALK* NSCLC by *EML4-ALK* fusion variant type ([*A*] v3 versus non-v3) and number of isoforms ([*B*] single versus multiple). Stratification analyses were further performed (*C*) to compare PFSs of the fusion variant types among patients with multiple isoforms and (*D*) to compare PFSs of different number of isoforms among patients with non-v3 *EML4-ALK* tumors. Num, number; OS, overall survival; PFS, progression-free survival.

significantly shorter PFS than patients with single-isoform tumors (median = 8.9 versus 15.9 mo) after treatment with the first-generation ALK inhibitor, crizotinib. Genomic breakpoints in *ALK* have been predominantly identified in the intron 19 of *ALK* and, interestingly, distributed evenly across the entire intron 19.[24] On its partner side, beyond *EML4*, chromosomal double-strand breaks involved in *ALK* rearrangement have been profoundly concentrated on the short arm of chromosome 2,[10,13] significantly associated with their proximity to *ALK* in the nucleus (chromosome 2 versus others: p value $= 1.7 \times 10^{-14}$).[9] Dual in-frame 3′ ALK rearrangements, namely two different gene partners fused with ALK and coexist in the same tumor, have been increasingly reported and cataloged,[13] and were found to be associated with poor overall and progression-free survivals in a relatively large Chinese NSCLC cohort.[25] In a blood-tissue matched analysis, 21% of patients with *ALK*-rearranged tumors were found to have different *EML4-ALK* variants between liquid (circulating tumor DNA) and tissue biopsies,[8] indicating the coexistence of various fusion variants in the same patient. In dramatic contrast to the rarity of fusion heterogeneity in tumor tissues detected at the genomic level,[6,10,13,25] our targeted deep RNA sequencing captured nearly half of *ALK*-rearranged advanced-stage clinical tumors harboring multiple-fusion isoforms. This high percentage was likely a result of the ability to capture a collection of heterogeneity at the genomic, RNA splicing, and epigenetic levels, including technical advantages in its open end (anchored on one end *ALK* only), high-enrichment efficiency (PCR versus hybrid capture), and use of near

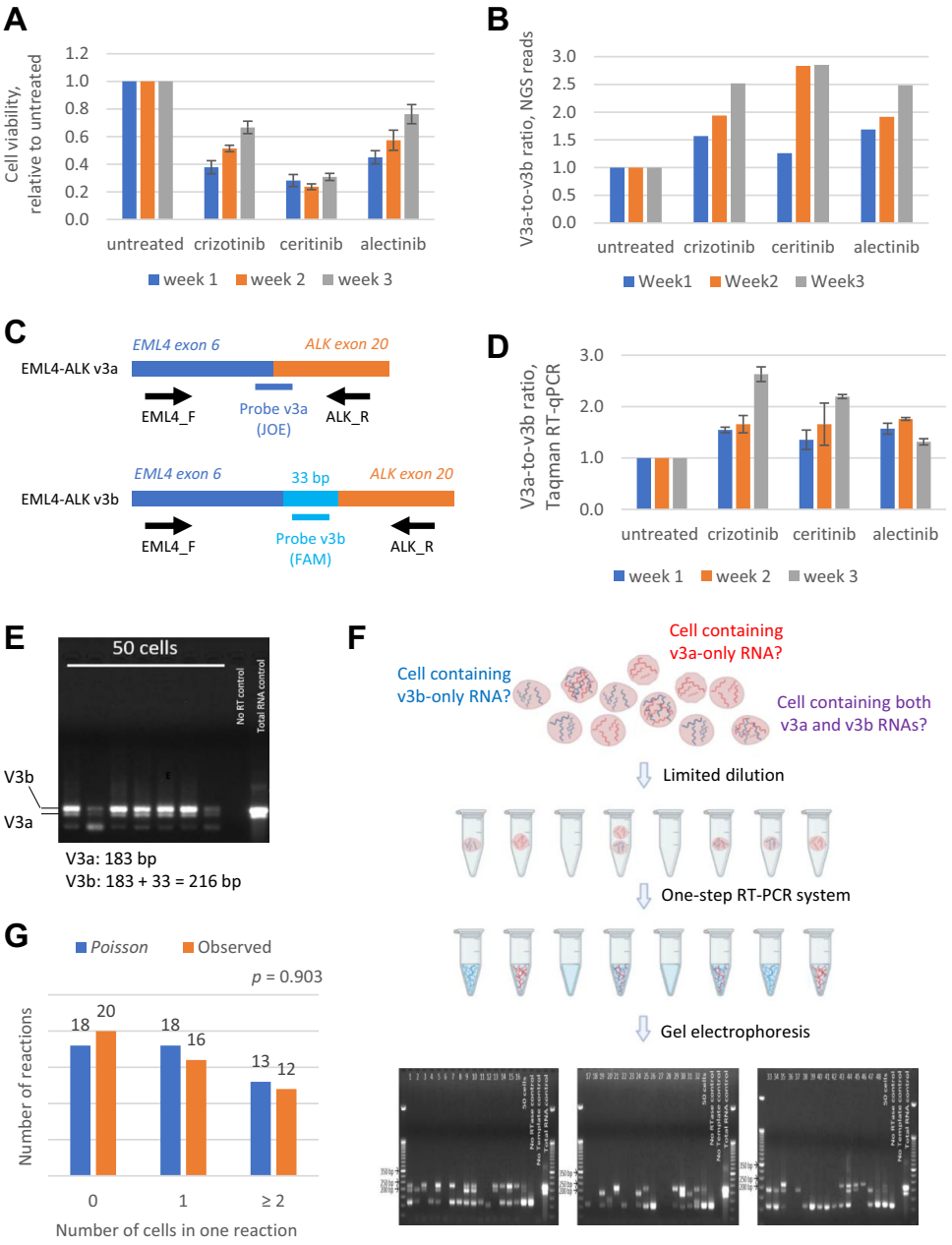

Figure 4. In vitro experiment evaluating the effect of *ALK* inhibitors crizotinib, alectinib, and ceritinib on *EML4-ALK* v3a and v3b fusion variant expression in the v3a- and v3b-expressing cell line H2228. (*A*) Cell viability of H2228 cells after treatments with TKIs for 1, 2, and 3 weeks (triplicates). (*B*) NGS data revealing the v3a-to-v3b ratios for H2228 cells after treatments with TKIs for 1, 2, and 3 weeks. (*C*) Schematic presentations for the v3a- and v3b-specific TaqMan RT-qPCR design. (*D*) The RT-qPCR results revealed the v3a-to-v3b ratios for H2228 cells after treatments with TKIs for 1, 2, and 3 weeks (using aliquots from the same samples as used in the NGS analyses in (*B*). (*E*) Direct cell-RT-PCR amplification for *EML4-ALK* v3 fusions using 50 H2228 cells, eight replicates. (*F*) A schematic diagram describing a limited dilution and direct cell-RT-PCR experiment. With the limited dilution down to one cell per reaction, the gel electrophoresis revealed that 20 reactions yielded no expected-size amplicon, eight yielded the v3a amplicon (expected 183 bp), eight yielded the v3b amplicon (expected 216 bp), and 12 yielded mixed amplicons. The two bands at approximately indicated v3a and v3b variant amplicons. (*G*) Comparing the numbers of reactions with 0, 1, and greater than or equal to 2 cells between expected by Poisson distribution and observed. bp, base pair; NGS, next-generation sequencing; RT-PCR, reverse-transcriptase polymerase chain reaction; RT-qPCR, reverse-transcriptase quantitative polymerase chain reaction; TKI, tyrosine kinase inhibitor.

exon-intron boundary PCR primers that are associated with high detection sensitivity even when mRNA in FFPE tissues is highly degraded.[16] In addition, our bioinformatics solution SplitFusion that can comprehensively map cryptic exon splicing also contributed to the high frequency of fusion heterogeneity captured in our study patients.

Different gene fusion partners to ALK may affect cellular locations of the fusion proteins,[24] hence they may have differed functions and associated clinical outcomes. Nevertheless, the mechanism underlying the poor clinical outcome in patients with multiple *EML4-ALK* isoforms in the same tumor, as opposed to the well-characterized evolving resistance point mutations,[14] is unknown. Insertions and deletions (in-frame) could lead to more profound protein structure and property changes than do point mutations.[26] Therefore, multiple-isoform–harboring tumors may express structurally diverse ALK proteins and easier to develop resistances to a single targeting agent than a uniform protein can. Interestingly, a patient was discovered to have relapse-response-relapse owing to evolved compound resistance mutations after sequential crizotinib and lorlatinib treatments and, interestingly, response to the less potent crizotinib again.[27] Although the occurrence of compound resistance point mutations is not very common, further studies are needed to investigate whether the *EML4* intronic region is a breakpoint "hot-zone" that may provide a high genetic plasticity for evolving resistant insertion and deletion clones along the course of targeted therapy.

Even among the "fine" variants v3a- and v3b-containg H2228 cells, our in vitro inhibition experiments using three different ALK inhibitors revealed an enrichment of the v3a-expressing cells, indicating v3a is more resistant to ALK inhibitors than v3b. This was consistent with previous study revealing higher half maximal inhibitory concentrations (IC50) of two ALK inhibitors (crizotinib and TAE684) for v3a than for v3b cells.[12] Our prolonged inhibition period over 3 weeks resulted in steady increased ratios of v3a-to-v3b over time for all the three inhibitors, further revealing the selection of less sensitive variant cells even among the seemingly homogenous H2228 cell line. This may explain the previous results on inhibition of H2228 across a wide range of ALK TKI concentrations,[5,24] which suggested heterogeneous responses among the H2228 cell population. Our single-cell RT-PCR result revealed that at least most H2228 cells express either v3a or v3b transcript in single cells, suggesting a non-stochastic expression that might be due to epigenetic regulations but requires further studies to fully elucidate the molecular mechanisms.

The length of the EML4-ALK protein was suggested to be associated with the protein stability and therefore may affect treatments of ALK inhibitors[12,24] and HSP40.[12,28] In our study, 20 patients belong to the short-protein group, including only one patient with the v5 fusion and 19 patients with v3 fusion (Table 1). Thus, the comparison of OS and PFS between patients with short and long proteins would be highly similar to those between patients with and without v3.

We have used an AMP-based targeted RNA-seq assay with ALK antisense primers that specifically enrich for potential fusions at the 5′ end of ALK kinase. The reciprocal fusions found in DNA-based NGS methods are likely passengers.[9] Although AMP can detect any 3′ fusion partners using sense primers, such as those *FGFR 1/2/3* gene fusions we detected by AMP previously,[16] our interest in ALK fusions has been focused on potential cancer drivers (5′ XXX-ALK 3′) and not on those reciprocal fusions (5′ ALK-XXX 3′). As *ALK* promoter is not active in lung tissue (transcript per million = 0.08),[29] the reciprocal fusions occurred at genomic levels will not be expressed into RNA and no method (RT-PCR, targeted RNA-seq, or whole transcriptome sequencing) would detect the nonexisting "reciprocal RNA" in NSCLC. For *ROS1* promoter that is active in lung tissue (transcript per million = 11.09),[30] reciprocal fusion RNAs may be present and detectable, although just passengers. The *ALK-XXX* formation at the genomic level detected by DNA assays might or might not be accompanied by functional driver *XXX-ALK* fusions; and when it is not, orthogonal diagnosis methods are needed before receiving ALK targeted therapy or other treatments.[9,10]

In conclusion, our findings suggest that fusion heterogeneity detected by RNA sequencing may inform treatments of patients with fusion-rearranged cancer. As our study size was rather small with only 51 recruited patients, larger studies are needed to validate our observations before fusion heterogeneity can be considered to stratify patients to receive potent target inhibitors upfront, such as lorlatinib with relatively higher-grade adverse events. Whether fusion heterogeneity associated with worse post-crizotinib survival can be extended to the second, third, and newer generations of TKIs remains to be evaluated.

CRediT Authorship Contribution Statement

Zhengbo Song: Conceptualization, Resources, Writing—Review and Editing, Funding acquisition.

Shifeng Lian: Formal analysis, Methodology, Writing—Review and Editing.

Silvia Mak: Investigation, Methodology, Writing—Review and Editing.

Maggie Zi-Ying Chow: Investigation, Methodology, Writing—Review and Editing.

Chunwei Xu, **Wenxian Wang, Yanqiu Gao, Wah Cheuk**: Resources.

Hoi Yee Keung, **Chenyu Lu**: Methodology, Writing—Review and Editing.

Firaol Tamiru Kebede: Methodology.

William Chi Shing Cho: Resources, Writing—Review and Editing.

Mengsu Yang: Supervision, Funding acquisition.

Zongli Zheng: Conceptualization, Methodology, Writing—Original Draft, Supervision, Funding acquisition.

Acknowledgments

The authors thank financial supports from the Ming Wai Lau Centre of Reparative Medicine of Karolinska Institutet (Lau Grant), the City University of Hong Kong (internal grant), the National Natural Science Foundation of China (81672098 to Dr. Zheng; 81802276 to Dr. Song), The Hong Kong Research Grants Council (11319516 to Drs. Yang and Zheng), The Innovation and Technology Fund of Hong Kong Government (ITS/344/15 to Dr. Zheng), and The Swedish Research Council (202001418 to Dr. Zheng).

Supplementary Data

Note: To access the supplementary material accompanying this article, visit the online version of the *Journal of Thoracic Oncology* at www.jto.org and at https://doi.org/10.1016/j.jtho.2021.09.016.

References

1. Soda M, Choi YL, Enomoto M, et al. Identification of the transforming EML4-ALK fusion gene in non-small-cell lung cancer. *Nature*. 2007;448:561-566.
2. Ou SI, Nagasaka M, Brazel D, Hou Y, Zhu VW. Will the clinical development of 4th-generation "double mutant active" ALK TKIs (TPX-0131 and NVL-655) change the future treatment paradigm of ALK+ NSCLC? *Transl Oncol*. 2021;14:101191.
3. Yoshida T, Oya Y, Tanaka K, et al. Differential crizotinib response duration among ALK fusion variants in ALK-positive non-small-cell lung cancer. *J Clin Oncol*. 2016;34:3383-3389.
4. Lin JJ, Shaw AT. Differential sensitivity to crizotinib: does EML4-ALK fusion variant matter? *J Clin Oncol*. 2016;34:3363-3365.
5. Woo CG, Seo S, Kim SW, et al. Differential protein stability and clinical responses of EML4-ALK fusion variants to various ALK inhibitors in advanced ALK-rearranged non-small cell lung cancer. *Ann Oncol*. 2017;28:791-797.
6. Lin JJ, Zhu VW, Yoda S, et al. Impact of EML4-ALK variant on resistance mechanisms and clinical outcomes in ALK-positive lung cancer. *J Clin Oncol*. 2018;36:1199-1206.
7. Zhang SS, Nagasaka M, Zhu VW, Ou SI. Going beneath the tip of the iceberg. Identifying and understanding EML4-ALK variants and TP53 mutations to optimize treatment of ALK fusion positive (ALK+) NSCLC. *Lung Cancer*. 2021;158:126-136.
8. Camidge DR, Dziadziuszko R, Peters S, et al. Updated efficacy and safety data and impact of the EML4-ALK fusion variant on the efficacy of alectinib in untreated ALK-positive advanced non-small cell lung cancer in the global phase III ALEX study. *J Thorac Oncol*. 2019;14:1233-1243.
9. Song Z, Lu C, Xu CW, Zheng Z. Noncanonical gene fusions detected at the DNA level necessitate orthogonal diagnosis methods before targeted therapy. *J Thorac Oncol*. 2021;16:344-348.
10. Li W, Guo L, Liu Y, et al. Potential unreliability of uncommon ALK, ROS1, and RET genomic breakpoints in predicting the efficacy of targeted therapy in NSCLC. *J Thorac Oncol*. 2021;16:404-418.
11. Davies KD, Le AT, Sheren J, et al. Comparison of molecular testing modalities for detection of ROS1 rearrangements in a cohort of positive patient samples. *J Thorac Oncol*. 2018;13:1474-1482.
12. Heuckmann JM, Balke-Want H, Malchers F, et al. Differential protein stability and ALK inhibitor sensitivity of EML4-ALK fusion variants. *Clin Cancer Res*. 2012;18:4682-4690.
13. Ou SI, Zhu VW, Nagasaka M. Catalog of 5' fusion partners in ALK-positive NSCLC circa 2020. *JTO Clin Res Rep*. 2020;1:100015.
14. Lin JJ, Riely GJ, Shaw AT. Targeting ALK: precision medicine takes on drug resistance. *Cancer Discov*. 2017;7:137-155.
15. Cai W, Lin D, Wu C, et al. Intratumoral heterogeneity of ALK-rearranged and ALK/EGFR coaltered lung adenocarcinoma. *J Clin Oncol*. 2015;33:3701-3709.
16. Zheng Z, Liebers M, Zhelyazkova B, et al. Anchored multiplex PCR for targeted next-generation sequencing. *Nat Med*. 2014;20:1479-1484.
17. Zheng Z, Shetty R, Liebers M, et al. A one-tube assay for simultaneous detection of gene mutation, fusion, copy number alteration and expression. *Cancer Res*. 2015;75(suppl 15):4895-4895.
18. Song Z, Xu C, He Y, et al. Simultaneous detection of gene fusions and base mutations in cancer tissue biopsies by sequencing dual nucleic acid templates in unified reaction. *Clin Chem*. 2020;66:178-187.
19. Bushnell B. BBMap. 37.75 version [software]. https://sourceforge.net/projects/bbmap/. Accessed September 14, 2021.
20. Kent WJ. BLAT—the BLAST-like alignment tool. *Genome Res*. 2002;12:656-664.
21. Li H, Durbin R. Fast and accurate long-read alignment with Burrows-Wheeler transform. *Bioinformatics*. 2010;26:589-595.
22. Huang J, Zheng Z, Andersson AF, Engstrand L, Ye W. Rapid screening of complex DNA samples by single-molecule amplification and sequencing. *PLoS One*. 2011;6:e19723.
23. Zheng Z, Advani A, Melefors O, et al. Titration-free massively parallel pyrosequencing using trace amounts of starting material. *Nucleic Acids Res*. 2010;38:e137.
24. Noh KW, Lee MS, Lee SE, et al. Molecular breakdown: a comprehensive view of anaplastic lymphoma kinase

(ALK)-rearranged non-small cell lung cancer. *J Pathol*. 2017;243:307–319.
25. Su Y, Long X, Song Y, et al. Distribution of ALK fusion variants and correlation with clinical outcomes in Chinese patients with non-small cell lung cancer treated with crizotinib. *Target Oncol*. 2019;14:159–168.
26. Vetter IR, Baase WA, Heinz DW, Xiong JP, Snow S, Matthews BW. Protein structural plasticity exemplified by insertion and deletion mutants in T4 lysozyme. *Protein Sci*. 1996;5:2399–2415.
27. Shaw AT, Friboulet L, Leshchiner I, et al. Resensitization to crizotinib by the lorlatinib ALK resistance mutation L1198F. *N Engl J Med*. 2016;374:54–61.
28. Richards MW, Law EW, Rennalls LP, et al. Crystal structure of EML1 reveals the basis for Hsp90 dependence of oncogenic EML4-ALK by disruption of an atypical β-propeller domain. *Proc Natl Acad Sci U S A*. 2014;111:5195–5200.
29. GTEx portal. Gene page: ALK. https://gtexportal.org/home/gene/ALK. Accessed September 14, 2021.
30. GT.Ex portal. Gene page: ROS1. https://gtexportal.org/home/gene/ROS1. Accessed September 14, 2021.